

FIG. 2. Experimental and calculated SDW<sup>3</sup> ratios of coincidence rates versus angle. Normalization of the ratios is arbitrary.

work, with the objective of reducing the various backgrounds, is in progress.

The authors would like to thank Dr. A. W. Overhauser for several helpful suggestions and for permission to use the calculated curves shown in Figs. 1 and 2.

†This research was partially supported by the National Science Foundation.

\*National Defense Education Act Fellow.

<sup>1</sup>A. W. Overhauser, *Phys. Rev. Letters* **13**, 190 (1964).

<sup>2</sup>A. W. Overhauser, *Bull. Am. Phys. Soc.* **10**, 339 (1965).

<sup>3</sup>A. W. Overhauser, private communication.

<sup>4</sup>A. T. Stewart, J. B. Shand, and S. M. Kim, *Proc. Phys. Soc. (London)* **88**, 1001 (1966).

<sup>5</sup>S. Berko and J. S. Plaskett, *Phys. Rev.* **112**, 1877 (1958).

## PHASE TRANSITION OF HARD-SQUARE LATTICE WITH SECOND-NEIGHBOR EXCLUSION\*

Francis H. Ree

Lawrence Radiation Laboratory, University of California, Livermore, California

and

Dwayne A. Chesnut

Shell Development Company, Houston, Texas

(Received 9 November 1966)

This report presents some evidences indicating a possible fluid-solid phase transition for a two-dimensionally infinite hard-square "lattice gas." The pair interaction between molecules is an infinite repulsion due to the finite geometrical size of molecules such that the nearest and second-nearest neighbors of a site occupied by the center of a molecule cannot be occupied by other molecules (see the shaded area in the inset of Fig. 1).

Recently, Kramers and Wannier's matrix method has been used rather extensively to investigate occurrence of an order-disorder transition on the square lattice which occurs when the interaction is limited to nearest-neighbor exclusion.<sup>1,2</sup> Bellemans and Nigam<sup>3</sup> applied it also to square-lattice systems with interactions extending up to third neighbors. With second-neighbor exclusion, their studies on semi-infinite strips ( $M \times \infty$ ) with width  $M$  ranging from 2 to 12 led to no definite conclusions regarding a thermodynamic phase transition for the limiting  $\infty \times \infty$  system, although a first-order phase transition seemed to be ruled out.

In an attempt to determine the location and

nature of this transition, therefore, we made similar studies with width extending up to  $M = 18$  with periodic boundaries. The following thermodynamic variables are calculated: the reduced pressure  $P^* [\equiv P/(kT)]$ ; the lattice constant is taken to be the unit of length,  $k =$  Boltzmann's constant;  $T =$  absolute temperature], the reduced density  $\rho^* [\equiv \rho/\rho_0; \rho_0 =$  the density at close packing  $= 0.25]$ ,  $d\rho/d\mu^* [\mu^* =$  the reduced chemical potential  $\equiv \mu/(kT)]$ , and  $d^2\rho/d\mu^{*2}$ . In the calculation, the quantity  $u \equiv z/(1+z)$  [ $z \equiv$  activity  $= \exp(\mu^*)$ ] is used as an independent variable. In this way, the interval  $(0, \infty)$  for  $z$  is mapped onto a finite interval  $(0, 1)$  for  $u$ . Furthermore, equal increments in  $u$  give approximately equal increments in the density except at the high-density end.

These thermodynamic variables are expressed exactly in terms of the eigenvalues  $\lambda_i$  and the corresponding eigenvectors  $\Psi_i$  of a particular submatrix  $B$  of the symmetric Kramers-Wannier matrix  $A$  which is required in computing the thermodynamic properties of a finite  $M \times N$  system. The use of the CDC 6600 for this stage of the calculation gives an accuracy of 9 digits or better for all the thermodynamic

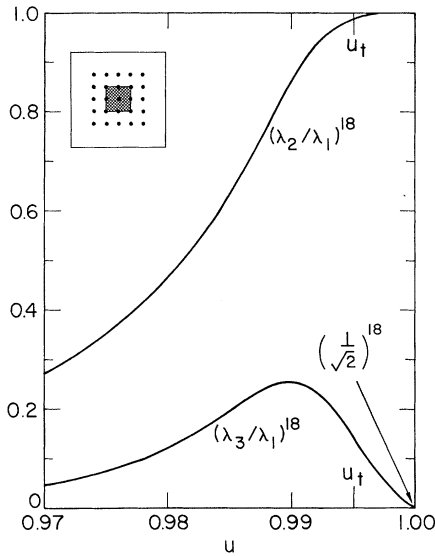


FIG. 1. Eigenvalue ratios ( $\lambda_1 > |\lambda_2| > \lambda_3$ ) of the matrix **B**; the largest eigenvalue  $\lambda_1$  gives the thermodynamic properties of an  $18 \times \infty$  hard-square lattice with the first- and the second-neighbor exclusion (see the inset).

variables reported. In this way errors arising from numerical differentiations are avoided.<sup>4</sup> The submatrix **B** belongs to the one-dimensional symmetric representation of the dihedral group of order  $2M$ , and its largest eigenvalue is also the largest eigenvalue  $\lambda_1$  of **A**. The knowledge of  $\lambda_1$  only is sufficient for computing the pressure for an  $M \times \infty$  system:  $P^* = M^{-1} \ln \lambda_1$ .

Furthermore, the knowledge of the eigenvalues and eigenvectors enables one to study the long-range correlations. In particular, long-range order occurs if at least two eigenvalues are "asymptotically" degenerate,<sup>2,5</sup> i.e.,

$$\lim_{M \rightarrow \infty} |\lambda_i / \lambda_1|^M \neq 0 \text{ for } i > 1.$$

For a semi-infinite system, the largest eigenvalue is always a nondegenerate and positive number for all positive, finite values of activity. However, the limiting behavior of  $|\lambda_i / \lambda_1|^M$  can be studied as a function of both  $z$  and  $M$  to provide still another way of locating the onset of long-range order.

In Fig. 1, these ratios are shown for two eigenvalues,  $\lambda_2 (< 0)$  and  $\lambda_3 (> 0)$ , with the next two largest moduli for the submatrix **B** for the case  $M = 18$ . In the case of the hard-square lattice with nearest-neighbor exclusion, the eigenval-

ue with the second largest modulus belongs to the submatrix for the one-dimensional anti-symmetric representation.<sup>2</sup> In the present case, however, the eigenvalues with the two largest moduli come from the submatrix **B** for the symmetric representation. The behavior of the eigenvalue spectrum of the present model resembles that of the square lattice with nearest-neighbor exclusion,<sup>2</sup> which itself is similar to the Ising model.<sup>5</sup> In particular, the transition point ( $u = u_t$ ) appears to be characterized by an infinite degree of asymptotic degeneracy, while the disordered ( $u < u_t$ ) and the ordered ( $u > u_t$ ) states are characterized, respectively, by 0 and 2 degrees of asymptotic degeneracy in the eigenvalues with largest moduli. However, the two hard-square models behave differently in the following two ways. Firstly, an infinite number of eigenvalues for an  $\infty \times \infty$  system are identically zero in the present model (for example, 110 out of the 209 eigenvalues in the case  $M = 18$ ), while no  $\lambda_i$ 's become zero for  $u > 0$  in the case of nearest-neighbor exclusion. Except  $\lambda_1$  and  $\lambda_2$ , the ratios  $\lambda_i / \lambda_1$  for the nonzero eigenvalues of the present model approach  $2^{-1/2}$  at close packing for any  $M$  (rather than 0 as was the case for the nearest-neighbor exclusions). The location and magnitude of the maximum in  $(\lambda_3 / \lambda_1)^M$  vary as the width of an  $M \times \infty$  system changes in the manner shown in Table I. From these data, the limiting value,

$$\lim_{M \rightarrow \infty} (\lambda_3 / \lambda_1)_{\max}^M,$$

is likely to be unity. Noting that  $(\lambda_3 / \lambda_1)^M$  should approach  $2^{-M/2}$  at close packing,  $u_t$  will, therefore, lie close to 0.99. For  $u > u_t$ , long-range order will set in, because

$$\lim_{M \rightarrow \infty} (\lambda_2 / \lambda_1)^M$$

Table I. Variation of the location and magnitude of the maximum in  $(\lambda_3 / \lambda_1)^M$  as the width of an  $M \times \infty$  system changes.

$M$	$10 \times u$	$10^2 (\lambda_3 / \lambda_1)_{\max}^M \ln M$
6	9.9316	4.9160
8	9.8931	3.0859
10	9.8843	2.4489
12	9.8856	2.1681
14	9.8900	2.0347
16	9.8952	1.9756
18	9.9003	1.9605

Table II. Thermodynamic variables for  $M \times \infty$  hard-square lattice systems and the ratios for the eigenvalues having the first three largest moduli obtained at the points where  $(d^2\rho/d\mu^{*2})$  exhibits a maximum and a minimum.

	$M$	$10u$	$10\rho^*$	$P^*$	$10^2 d\rho/d\mu^*$	$10^2 d^2\rho/d\mu^{*2}$	$10(\lambda_2/\lambda_1)^M$	$10(\lambda_3/\lambda_1)^M$
$(d^2\rho/d\mu^{*2})_{\max}$	8	9.6039	8.7810	0.875 33	1.8908	-0.387 47	4.7908	0.8865
	10	9.7134	8.9309	0.944 16	1.7871	-0.260 85	5.2713	1.1527
	12	9.7741	9.0343	0.995 74	1.7120	-0.158 00	5.6777	1.3999
	14	9.8111	9.1072	1.035 00	1.6511	-0.076 83	5.9997	1.6206
	16	9.8357	9.1613	1.065 95	1.5971	-0.017 32	6.2564	1.8174
	18	9.855(3) <sup>a</sup>	9.2113	1.094 02	1.5473(3)	+0.020(1)	6.5432	2.0265
$(d^2\rho/d\mu^{*2})_{\min}$	6	9.8522	9.5155	1.119 56	1.1121	-0.742 94	8.2969	1.7065
	8	9.8858	9.5765	1.168 42	1.0989	-0.906 57	8.7735	1.8748
	10	9.8989	9.5855	1.190 32	1.1262	-1.045 44	9.0064	1.9779
	12	9.9068	9.5822	1.205 27	1.1516	-1.149 68	9.1496	2.0725
	14	9.9126	9.5762	1.217 65	1.1664	-1.219 99	9.2476	2.1665
	16	9.9173	9.5706	1.228 79	1.1693	-1.260 36	9.3201	2.2605
	18	9.9212(1)	9.5659	1.238 85	1.1648(3)	-1.277(1)	9.3744	2.3562

<sup>a</sup>9.855(3)  $\equiv$  9.855  $\pm$  0.003. See Ref. 4.

apparently does not vanish.

Next, the nature of a thermodynamic phase transition which may be associated with the occurrence of long-range order is investigated. We found that there occurs a maximum followed immediately by a minimum in the quantity  $d^2\rho/d\mu^{*2}$  for  $u$  near  $u_t$ . Table II tabulates the thermodynamic variables, as functions of  $M$  along the two trajectories: (i)  $(d^2\rho/d\mu^{*2})_{\max}$  and (ii)  $(d^2\rho/d\mu^{*2})_{\min}$ . In Fig. 2(a) the quantity  $d^2\rho/d\mu^{*2}$  is plotted as a function of both  $u$  and  $M$ . For large  $M$ , both Fig. 2(a) and Table II indicate that the difference  $\Delta(d^2\rho/d\mu^{*2}) [\equiv (d^2\rho/d\mu^{*2})_{\max} - (d^2\rho/d\mu^{*2})_{\min}]$  of the two extrema grows; however, the separation  $\Delta u [\equiv u_{\min} - u_{\max}]$  diminishes. In Fig. 2(b), these differences are plotted as a function of inverse powers of  $M$ . The difference  $\Delta(d^2\rho/d\mu^{*2})$  appears to level off when plotted against either  $M^{-1}$  or  $(\ln M)^{-1}$ . Although a stronger continuous transition, as was observed in the case of the nearest-neighbor exclusion, cannot be entirely ruled out, the extrapolation of the above results indicates that there may be a third-order phase transition with a discontinuous jump in  $d^2\rho/d\mu^{*2}$  at  $u = u_t$ , and that  $d\rho/d\mu^*$  (which is proportional to the compressibility) exhibits a cusp at  $u = u_t$ .

The above conclusion is based on an assumption that the thermodynamic quantities for larger systems ( $M \geq 20$ ) are similar in behavior to the cases for  $M \leq 18$  in the neighborhood of the transition point. The analysis of the data obtained in the present work indicates that the thermodynamic variables converge regularly for  $u < 0.95$  ( $\rho^* \leq 0.84$ ). In fact, the grand ca-

nonical partition function for an  $M \times \infty$  system reproduces correctly the first  $M-1$  fugacity ( $b_l$ ) and virial ( $B_l$ ) coefficients of the pressure for an  $\infty \times \infty$  system.<sup>2</sup> Unlike the lattice gas with the nearest-neighbor exclusion, however, the present model does not possess a well-defined sublattice structure. For example, even at the density of close packing, there are configurations with molecules occupying sites along a column of an  $M \times \infty$  system which can be rotated by one lattice site without affecting molecules occupying the adjacent columns. This type of freedom contributes an additional term,  $\ln 2/(2M)$ , to  $P/kT$  at high density. This term is the next significant part of the difference between  $P/kT$  and the dominant term,  $\frac{1}{4} \ln z$ , for high density. In fact, Bellemans and Nigam<sup>3</sup> showed that  $P/kT - \frac{1}{4} \ln z$  for an  $M \times \infty$  system and an  $\infty \times \infty$  system have different expansion parameters for large  $z$ , the former being  $z^{-1}$  and the latter being  $z^{-1/2}$ , and that the  $z^{-1}$  expansion for a semi-infinite system breaks down as  $M$  becomes infinite. Further clarification of this point comes from considering the eigenvalues of  $\mathbf{B}$  for  $M \leq 18$ . For large  $z$ ,

$$\lambda_1 \sim 2^{\frac{1}{2}} z^{M/2} [1 + az^{-1} + \dots]$$

and

$$\lambda_2 \sim -2^{\frac{1}{2}} z^{M/2} [1 + az^{-1} + \dots],$$

while the other nonzero  $\lambda_i$ 's behave as  $\lambda_i \sim z^{M/2} [\pm 1 + a_1 z^{-\frac{1}{2}} + \dots]$ . In the thermodynamic limit for an  $M \times M$  system, the contributions by the latter eigenvalues [there are asymptotically  $(1.618)^M$  of them] to the pressure, therefore, dominate at large  $z$ , although none of these

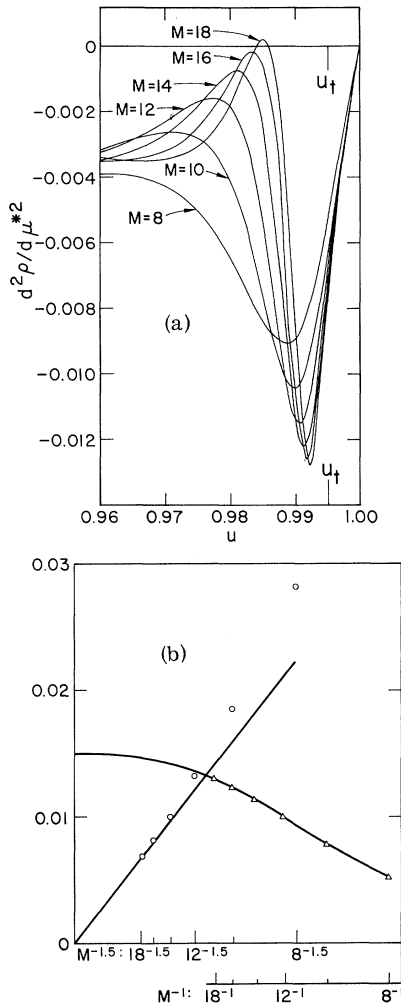


FIG. 2. (a) Plot of  $d^2\rho/d\mu^{*2}$  vs  $u$  for  $M \times \infty$  systems of hard-square lattices ( $M=8, \dots, 18$ ). (b) The differences ( $u_{\min} - u_{\max}$ ) of the position of the extrema of  $d^2\rho/d\mu^{*2}$  observed in (a) are plotted against  $M^{-1.5}$  as circles; the differences  $(d^2\rho/d\mu^{*2})_{\max} - (d^2\rho/d\mu^{*2})_{\min}$  are plotted against  $M^{-1}$ , as triangles.

eigenvalues becomes asymptotically degenerate to  $\lambda_1$ . The nonuniform convergence of the pressure for an  $M \times \infty$  system to that of an  $\infty \times \infty$  system may alter the location as well as the nature of the predicted transition. However, systems with relatively small  $M$  ( $\leq 18$ ) may still furnish enough information to establish a trend for the differences such as  $u_{\min} - u_{\max}$  and  $(d^2\rho/d\mu^{*2})_{\max} - (d^2\rho/d\mu^{*2})_{\min}$  in the neighborhood of the transition point. Under this assumption, we obtain the following values for thermodynamic variables at the transition point: from  $(d^2\rho/d\mu^{*2})_{\max}$  data,

$$u_t = 0.995 \pm 0.02 \quad (\text{or } \mu_t^* = 5.3 \pm 0.5),$$

$$P_t^* = 1.4 \pm 0.2,$$

$$(d\rho/d\mu^*)_t = 0.010 \pm 0.003,$$

$$(d^2\rho/d\mu^{*2})_{\max} = 0.0016 \pm 0.0003;$$

from  $(d^2\rho/d\mu^{*2})_{\min}$  data,

$$(d^2\rho/d\mu^{*2})_{\min} = -0.0134 \pm 0.002,$$

$$\lambda_3/\lambda_1 = [-(4.43 \pm 0.09)/(M \ln M)] \text{ for } M \gg 20;$$

from both sets of data,

$$\rho_t^* = 0.953 \pm 0.002,$$

$$(d^2\rho/d\mu^{*2})_{\max} - (d^2\rho/d\mu^{*2})_{\min}$$

$$= 0.0155 \pm 0.0005,$$

$$\lambda_2/\lambda_1 = -1 \quad (M \rightarrow \infty).$$

The value of  $P/\rho kT$  at the transition point increases from 2.15 to 5.9 as the exclusion of the hard-square lattice extends from nearest neighbors to the second neighbors. The corresponding molecular dynamics value<sup>6</sup> for hard disks is 10.13. Likewise, the value of  $B_2\rho_t$  changes from 0.92 to 1.07, while  $B_2\rho_t$  is estimated to be 1.38 for hard disks. However, the order of transition may change irregularly as was observed in both the hard-square lattice<sup>1-3</sup> and the hard-triangular lattice.<sup>7</sup> If the mesh size of the lattice becomes finer and the shape of molecules on sites is chosen to approximate shape of hard disks, agreement in thermodynamic values between the lattice and hard-disk systems should become closer.<sup>8</sup>

\*This work was performed under the auspices of the U. S. Atomic Energy Commission.

<sup>1</sup>L. K. Runnels, Phys. Rev. Letters **15**, 581 (1965). For a different approach, see D. A. Gaunt and M. E. Fisher, J. Chem. Phys. **43**, 2840 (1960).

<sup>2</sup>F. H. Ree and D. A. Chesnut, to be published.

<sup>3</sup>A. Bellemans and R. K. Nigam, Phys. Rev. Letters **16**, 1038 (1966); and to be published.

<sup>4</sup>The data on  $d\rho/d\mu^*$  and  $d^2\rho/d\mu^{*2}$  for an  $18 \times \infty$  system are, however, extrapolated from the finite difference formula for these quantities using several different  $\Delta u$ .

<sup>5</sup>J. Ashkin and W. E. Lamb, Jr., Phys. Rev. **64**, 159 (1943); L. Onsager, Phys. Rev. **65**, 117 (1944).

<sup>6</sup>B. J. Alder and T. E. Wainwright, Phys. Rev. **127**, 359 (1962).

<sup>7</sup>D. A. Chesnut, unpublished result.

<sup>8</sup>W. G. Hoover, B. J. Alder, and F. H. Ree, J. Chem. Phys. **41**, 308 (1964).